2017

Wet-Spun Biofiber for Torsional Artificial Muscles

Azadehsadat Mirabedini
University of Wollongong, am707@uowmail.edu.au

Shazed Md Aziz
University of Wollongong, shazed@uow.edu.au

Geoffrey M. Spinks
University of Wollongong, gspinks@uow.edu.au

Javad Foroughi
University of Wollongong, foroughi@uow.edu.au

Publication Details

Mirabedini, A., Aziz, S., Spinks, G. M. & Foroughi, J. (2017). Wet-Spun Biofiber for Torsional Artificial Muscles. Soft Robotics, 4 (4), 421-430.

Wet-Spun Biofiber for Torsional Artificial Muscles

Abstract
The demands for new types of artificial muscles continue to grow and novel approaches are being enabled by the advent of new materials and novel fabrication strategies. Self-powered actuators have attracted significant attention due to their ability to be driven by elements in the ambient environment such as moisture. In this study, we demonstrate the use of twisted and coiled wet-spun hygroscopic chitosan fibers to achieve a novel torsional artificial muscle. The coiled fibers exhibited significant torsional actuation where the free end of the coiled fiber rotated up to 1155 degrees per mm of coil length when hydrated. This value is 96%, 362%, and 2210% higher than twisted graphene fiber, carbon nanotube torsional actuators, and coiled nylon muscles, respectively. A model based on a single helix was used to evaluate the torsional actuation behavior of these coiled chitosan fibers.

Disciplines
Engineering | Physical Sciences and Mathematics

Publication Details
Mirabedini, A., Aziz, S., Spinks, G. M. & Foroughi, J. (2017). Wet-Spun Biofiber for Torsional Artificial Muscles. Soft Robotics, 4 (4), 421-430.

Wet-Spun Biofibre for Torsional Artificial Muscles

*Azadeh Mirabedini, Shazed Aziz, Geoffrey Spinks, Javad Foroughi**

ARC Centre of Excellence for Electromaterials Science, Intelligent Polymer Research Institute, AIIM Facility, University of Wollongong, Fairy Meadow, NSW 2519, Australia

Abstract

The demands for new types of artificial muscles continue to grow and novel approaches are being enabled by the advent of new materials and novel fabrication strategies. Self-powered actuators have attracted significant attention due to their ability to be driven by ambient environment including moisture. Despite continuous improvements production of biomaterial as artificial muscles still faces challenges. Here, we demonstrate the use of twisted and coiled wet-spun chitosan fibres to achieve a novel torsional artificial muscle. The coiled fibres exhibited significant torsional actuation where the free end of the coiled fibre rotated up to 1155 degrees per mm of coil length when hydrated. This value is 96%, 362% and 2210% higher than twisted graphene fiber, carbon nanotube torsional actuators and coiled nylon muscles, respectively. A model based on a single helix was used to evaluate the torsional actuation behaviour of these coiled chitosan fibres. The cytocompatiblity of coiled and untwisted fibres was evaluated by using skeletal muscle cell line. Cell viability, adhesion and differentiation onto the fibres were characterized by using calcein staining and confocal microscopy. The obtained results suggest that the structures may be useful as potential torsional bio-actuators for developing artificial muscles which are likely to find applications as 3D tissue scaffolds capable of muscles and nerves regenerations.

Keywords: *chitosan fibres, twisting, artificial muscle, chemical actuation, bio-actuator*

1. Introduction

Inspired by the outstanding capabilities of soft plant and animal structures researchers have developed soft active materials (SAM)[1] that mimic the remarkable features of life: movements in response to stimuli.[2] SAMs are capable of large deformation in response to a range of stimulus.[1] Artificial muscles based on this principle are of growing interest [3] converting the chemical potential of the environment into a mechanical response.[4,5] The use of soft materials can potentially provide devices with appropriate mechanical, chemical and biological properties that may even support cell growth and maintenance and certain cells are known to respond to mechanical stimuli.[6,7]

Thus far, a number of soft materials have been used as muscles including elastomers, conducting polymers, and ionically conducting polymers.[2] Stimuli-responsive hydrogels, three-dimensional covalently crosslinked polymer networks capable of accommodating large amounts of water,[8,9] provide the possibility for designing soft muscles sensitive to environmental stimuli.[10–12] The primary advantage of hydrogels is represented by their inherent responsiveness to extremely low driving voltages.[13] Additionally, these materials can use biologically relevant electrolytes making them well suited for applications within biology.[12,14] Another unique characteristic of biomimetic hydrogels is that they undergo huge volume changes, which occur in relatively narrow ranges of changes of temperature, pH, and ionic strength.[12,15]

Plants generate many different kinds of movement in response to a wide range of signals(e.g. light, gravity, water and chemicals) within different timescales even though they lack muscles.[16] These movements are not driven by energy released from metabolic processes but solely by physical mechanisms. The mechanical responsiveness in many plants is also known to be produced by helical organizations of cellulose microfibrils.[17] For example, torsional movements such as helical motion of tendrils[18] and twisting of wood cells[19] are generated by swelling or shrinkage in different parts of the tissue in response to a change in humidity. Whist researchers have also distinguished active and passive systems among plant movements,[20] animals are typically involved in active movements upon stimulation whereby live tissues and cells can actively deform in response to the stimuli. Looking into our body, several reactions and processes could be also found from varieties of organs in response to electrical signals travelling down a nerve cell to them like muscle contraction as a result of calcium release and storage.[21] Mechanical stimulation has shown to have a vital control over morphology, proliferation, lineage commitment, and differentiation of cells.[22,23] Researchers previously documented cellular responses to stretching toward mechanical signalling.[24,25] Still, there are inadequate results on cell response to torsional stimulus. Cells will probably go through “cellular mechanotransduction” upon stimulation; a term refers to the processes by which cells convert physical forces into changes in intracellular biochemistry.[26] Cells are composed of an interconnected network of tensed cables and membranes. These transmembrane receptors may function as mechanoreceptors that provide a preferred path for mechanical force transfer across the cell surface.[26] Cellular responses to mechanical stimulus may vary by cell type and loading mode an also depend on the properties of extracellular

matrix (ECM) and the presence of soluble factors. Therefore, inducing mechanical in soft actuators has been of interest in recent years.

Motivated by lessons from nature, a few torsional actuators were also reported which respond to solvents and vapours.[27,28] To mimic muscles, soft and wet polymers able to interact with ions are required as mentioned. Hydrogels have shown that they can undergo huge deformations due to moisture ingress. This macroscopically swelling is controlled by the balance of free energy for the network expansion induced by transporting of ions which depends on the cross-linking density and interactions between polymer chains and solvents.[10,12] However, the macroscopic applications of hydrogels are limited in some cases due to the slow rate of solvent diffusion into the gel when swelling or deswelling.[33] To overcome this problem, hydrogels have been developed at micrometre length scale through different methods such as photolithography techniques[29–31] and fibre spinning.[32–34] Chitosan is a nontoxic semi-synthetic polyelectrolyte hydrogel[35,36] known as a well-established material for the fabrication of artificial muscles, as it undergoes a large volume change in response to a change in pH.[37] Apart from its nontoxic nature, chitosan is important because of its bioactivity, biocompatibility and its ability to adsorb and bind water. The tensile actuation properties of chitosan during pH changes have been previously studied. However, there still remained limitations in regard to the performance of hydrogel actuators such as their response time, very low and high pH and fabrication process.[38] The resulting capabilities of hydrogel actuators are not fully developed, yet. Herein, we found of the use of highly coiled chitosan fibres to function as torsional muscles for the first time. These coiled biofibres have been characterized properly with a view to improve both mechanical and biological properties. The ability to change the structure through chemical actuation affects by ion exchange and/or swelling of the coiled chitosan fibre will be used to change scaffold dimensions, giving rise to a tuneable device.

2. Experimental

2.1. Materials and Method

Chitosan of medium molecular weight (4.5 x 10^5 Da) with a degree of deacetylation of about 80.0% was obtained from Sigma-Aldrich (Australia). Acetic acid was supplied from Ajax Finechem (Australia) and used as provided. Sodium hydroxide pellets (Ajax Finechem) was

used as the coagulating agent. Phosphate buffered saline (PBS) tablet were purchased from Sigma-Aldrich (Australia).

2.2. Fabrication of Highly Twisted/Coiled Chitosan Muscles

For preparing the chitosan solution needed for the purpose of fibre spinning, 3% (w/v) of chitosan powder was dissolved in water containing 2.5% acetic acid and the solution was stirred at a temperature of ~50˚C overnight to form a homogenous solution. This solution was then filtered and precipitated using custom-made rotary wet-spinning equipment in a bath of aqueous 1M sodium hydroxide (Ethanol/H_2O: 1/4). These fibres were washed several times and stored in MilliQ water. To fabricate twisted and coiled fibres, two custom-made rotors with adjustable distance were employed which rotate in opposite directions. Wet fibres were suspended between two rigid supports fixed at both ends and kept straight during the twisting process. When the rotors start spinning in opposite directions, a symmetric twist was inserted into the fibre which causes the length to shorten.[27,39] Additionally, mechanical twisting makes the fibre become dehydrated but able to maintain a uniform pattern. At the critical point, a loop or coil developed in the structure which increased in number by further twisting. This process provides two dissimilar fibrillar structures comprising highly twisted and coiled helical chitosan fibres.

Additionally, to investigate the mechanism of torsional actuation, a ~340µm-diameter mandrel-made coiled fibre was produced by inserting twist in the wet fibre followed by coiling it around a metal mandrel. The structure was then thermally annealed to hold its shape and used in dry and fully hydrated states for calculations related to the helix model.

2.3. Characterization Methods

2.3.1. Microscopic observation

As-prepared wet-spun and dried coiled fibres were observed and photographed using a LEICA M205 stereomicroscope equipped with a LAS 4.1 software. Fibre diameters were measured from the taken images.

2.3.2. Morphological observation in wet and dry-state

The morphological structures of the fire surface and cross-sections were observed with JEOL JSM-7500 FESEM in dry-states.

Already dried samples were prepared by cutting cross sections in liquid nitrogen using a scalpel blade for imaging. They were then coated with a thin (15 nm) layer of platinum (Pt) to

aid with imaging and minimise beam heating effects. Cross sections were analysed at 25 kV accelerating voltage and a spot size setting of 12.

2.3.3. Mechanical Properties

Tensile tests were performed on a Dynamic Mechanical Tester (EZ-L Tester from Shimadzu, Japan), at 2 mm/min and a gauge length of 11.5 mm for untwisted, twisted and highly coiled fibres. Average values of tensile strength and maximum strain were determined after repeating the test four times. All types of fibres were assumed to have a rod-shape cross-section.

2.3.4. Chemically fuelled torsional actuation tests

Torsional actuation test (free of any external load) was performed by immersing a small chitosan fibre segment (20mm in length) in a beaker while one end of the fibre was clamped and the bottom end was free to rotate (as schematically shown in Figure 1). A rubber paddle (~500 times heavier than the fibre) was attached to the free rotating end to enhance the visibility of the fibre rotation which was recorded by a microscopic camera system (ISSCO-OPTEK).Water and ethanol was applied to the top of the fibre using a fine pipette for swelling (water) and deswelling (ethanol) experiments, respectively (See Movie S1 The Supporting Information). Three subsequent hydration/dehydration cycles were conducted to assess the reproducibility and reversibility of actuation profile. In addition to the free rotating tests, a reversible system was also developed by attaching a 50µm diameter nylon fibre to the paddle to act as a return spring. The other end of the nylon fibre was connected to a lever arm force/distance transducer (Aurora 300B) to apply a constant tensile force to the sample.

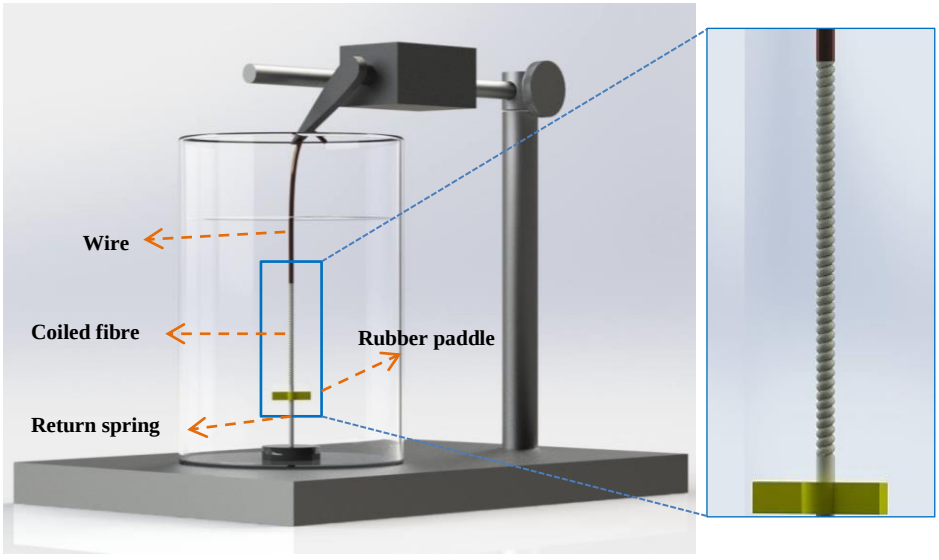

Figure 1 A schematic diagram illustrating the torsional actuation setup using a return spring fibre and a force / distance transducer to apply a constant tensile force and detect and changes in sample length.

2.3.5. In-vitro Bioactivity Experiments

The cytotoxicity, biocompatibility and proliferation of cells on the untwisted and coiled fibres were determined for primary myoblast muscle cell line (Rosa, kindly donated by Prof. Robert Kapsa, San Vincent Hospital, Australia)[40] without adding extra-cellular matrices to the fibers. Prior to use fibres in cell culture, about 30 mm lengths of fibers were fixed onto microscope slides with 4-well chamber wells (Lab TekRII, Thermo Fisher Scientific) glued on top which were then allowed to get dry overnight. Then, the samples underwent a sterilization process consisted of two washes in sterile condition of 70% ethanol (each for 30 minutes) and then four washes (each for 30 minutes) in sterile phosphate buffered saline (PBS, Sigma). Finally, they were kept in cell culture media overnight to remove all excess acid used during fibers production.

Myoblast cells were seeded at $5x10^5$ cells/cm^2 in a proliferation medium containing Ham's F-10 medium (Sigma), supplemented with 2.5 ng/mL bFGF (Peprotech) and 20% fetal bovine serum (FBS, Invitrogen supplied by Life Technologies), and 1% 1% penicillin/streptomycin (P/S, Life Technologies). This medium was changed to the differentiation medium after 24 hours in culture (50-50 mixture of Dulbecco's modified Eagle's medium (DMEM, Life Technologies) and F-12 medium (DMEM/F12, Life Technologies) supplemented with 3% FBS and 1% P/S). The cells were left and allowed to differentiate for 4 days in the media. Cell morphology was assessed after 5 days in three independent experiments containing four samples each. Myoblast cells were stained by addition of calcein AM (Invitrogen) solution at a final concentration of 5µM (1:200 dilution) and incubated at 37 ºC for 10 mins. Image analysis was performed using Leica TSC SP5 II microscope.

3. Results and discussion

3.1. Morphology of as-prepared chitosan fibres

Stereomicroscope and SEM images of hydrated and dry as-spun, wet-spun untwisted, twisted and coiled chitosan fibres are shown in Figure 2 (a-g). The untwisted fibres in the wet-state are shown to be uniform in diameter and straight opaque structures with an average diameter of ~700 ± 30 µm as displayed in Figure 2 (a). Cross-sections of dried spun fibres in Figure 2(d) clearly show the cylinder shaped form of the chitosan fibres which appeared pore-free.

While twisting the fibres in wet-state using rotors, a symmetric twist was inserted into the fibre which causes fibre dehydration and a decrease in diameter (Figure 2 (b)). Coils start to be developed in the structure at a critical point and increase in number by further twisting (Figure 2 (c)). It was noticed that the transparency of the fibres was improved after being dried suggesting that the water-swollen, untwisted chitosan fibres were microscopically heterogeneous.

As evident from SEM images, the twisted fibres remained twisted after drying. Meanwhile, the coiled fibres demonstrated a regular helical structure as depicted in Figure 2 (g) with diameters of ~190±10 µm when dried. A spiral shape can be seen for the cross- section of coiled chitosan fibres as shown in Figure 2 (e).

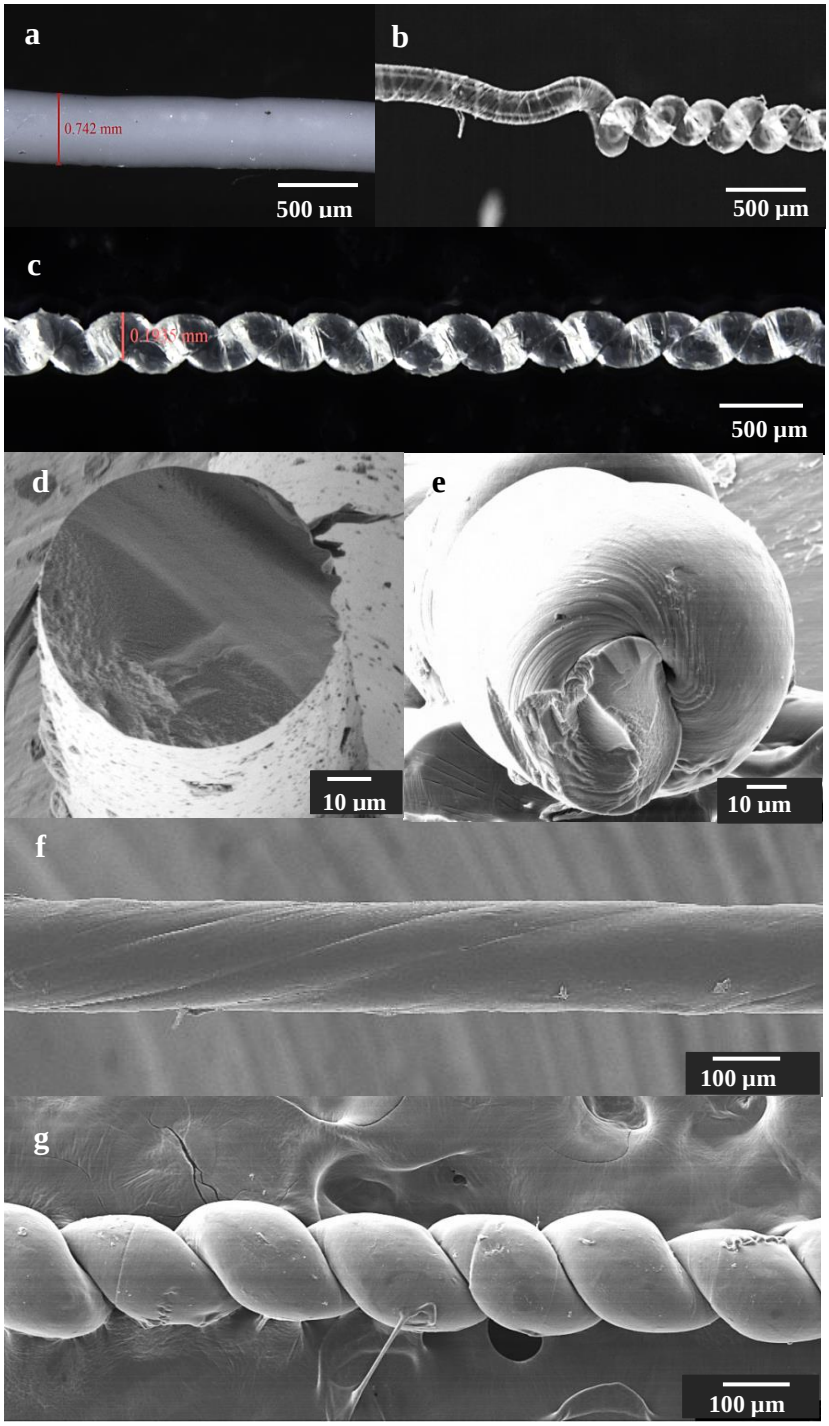

Figure 2 Stereomicroscopic images of (a) opaque wet, (b) dried twisted and (c) transparent helical structure of dry coiled chitosan fibres. SEM micrographs of cross-sections of (d) uncoiled, (e) coiled and surface of (f) twisted and (g) coiled dry chitosan fibres

3.2. Mechanical Properties

Stress-strain curves were obtained for neat, twisted and coiled chitosan fibres to examine their mechanical properties. These properties were tested at room temperature in the dry-state and the averages of the three specimens tested are given in Table 1.

Table 1 Mechanical property of neat, twisted and coiled chitosan fibres

Fibre Name	Young's Modulus (GPa)	Stress at Break (MPa)	Strain at Break (%)
Untwisted fibre	1.89±0.58	37.33±2.15	14.18±0.89
Twisted fibre	0.97±0.25	7.54±1.4	15.03±1.56
Coiled fibre	0.39±0.12	12.61±1.58	20.38±1.35

Stress–strain curves obtained from the dried untwisted, twisted and coiled chitosan fibres show a significant decrease in robustness of the latter. Young's moduli of fibres were shown to be ~1.89 GPa, ~0.97 GPa and 0.39 GPa for the neat, twisted and coiled chitosan fibres, respectively. Coiling significantly reduces axial stiffness due to their spring-like nature. These data were calculated assuming that the cross-sectional area was circular with a diameter equal to the widest part of the coiled fibre. Analysis of these curves also indicated a stress at break of ~37.3 MPa with ~14.1 % strain for neat chitosan fibres compared with only ~7.54 MPa and 12.61 MPa stress with ~15% and ~20.4% strain for twisted and coiled fibres, respectively. The results indicate that the twisting process will decrease the Young's modulus and ultimate stress while increasing the ultimate strain. This outcome can be possibly due to the change in polymer chain orientation from along the fibre axis (untwisted) to a helical conformation in the twisted structure.

3.3. Chemically fuelled torsional actuation results

3.3.1. Free torsional actuation of chitosan fibres

Figure 3 compares the water-fuelled torsional actuation shown by neat, twisted, mandrel-coiled and fully coiled chitosan fibres, respectively. The experiments were repeated 4 times for each sample until reaching a reproducible response. The neat untwisted fibre did not generate any torsional actuation, while the twisted and mandrel-coiled chitosan fibres have shown similar non-reversible untwisting when hydrated. Dehydration in ethanol removes the water from the fibre but did not reverse the swelling-induced untwisting. Table 2 shows the changes in weight of the fibres when subjected to the swelling/deswelling process.

Table 2 Changes in weights of fabricated fibres in dry and wet conditions

Fibre Condition	Twisted Fibre (mg)	Mandrel-Coiled Fibre (mg)	Self-Coiled Fibre (mg)
Dry state	1.12	0.92	1.24

Wet state (water)	2.74	1.58	3.0
Wet state (ethanol)	1.21	1.05	1.52
Dry state after ethanol charging	1.14	0.96	1.28

The lack of reversibility in the torsional actuation of the twisted and mandrel coiled fibres is likely due to the hydration-induced recovery of polymer chain orientation generated in the initial twisting / drying process. Hydration produces a gel-like state in the chitosan and allows the oriented polymer chains to regain their preferred random conformation. The shrinkage caused by dehydration of the fibres does not generate a driving force to re-twist the fibres. Consequently, the torsional actuation of the twisted and mandrel coiled chitosan fibres is not reversible in the current configuration.

In contrast, the overtwisted chitosan fibre showed some reversibility in the torsional actuation. A paddle rotation of more than 33 full turns (12,000°) was produced (Figure 3) by a free rotating coiled chitosan fibre through the swelling process. In this free rotation configuration a re-twisting of approximately 40% of the untwisting was observed on dehydration. The partial reversibility of the torsional actuation of these over-twisted fibres suggests a permanency of the coiled structure, perhaps due to yielding during twist insertion and coiling as occurs in semi-crystalline polymer fibres.[39]

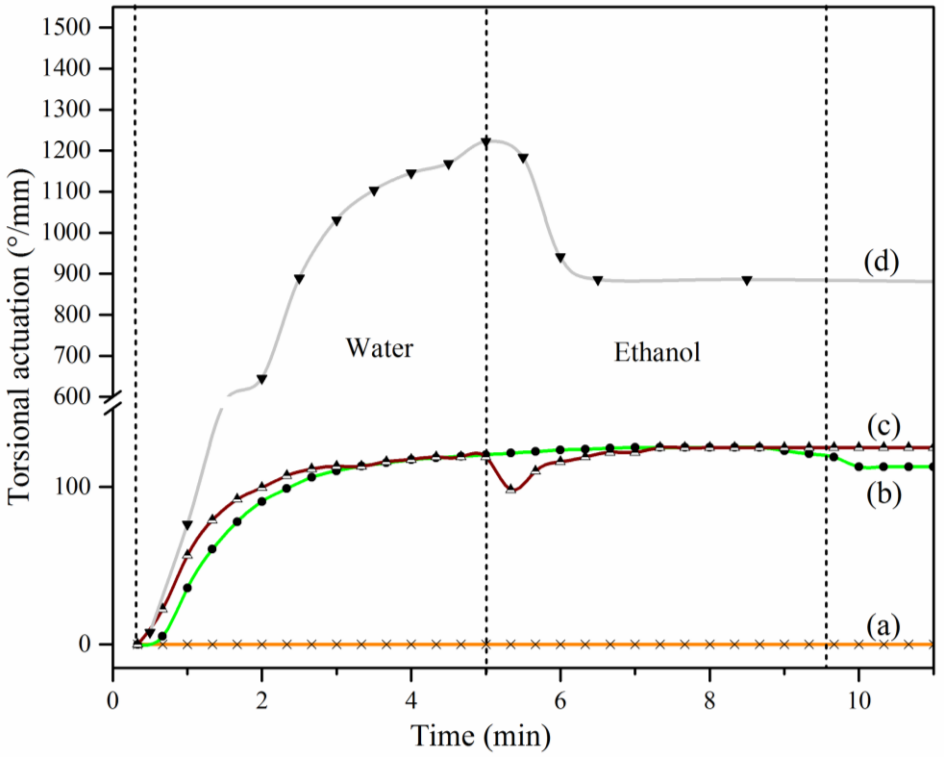

Figure 3 Comparison of torsional actuation and reversibility of (a) untwisted, (b) twisted, (c) mandrel-coiled and (d) coiled chitosan fibres

3.3.2. Reversible torsional actuation of coiled chitosan fibres

Previous work has shown that the reversibility of torsional actuation can be improved by operating the torsional actuator against a torsional return spring.[41] Figure 4 shows the torsional actuation of coiled chitosan structures using different lengths of return spring fibre together with the results obtained from free rotation (without a return spring). Three swelling/deswelling cycles were conducted for each type of torsional actuator. Swelling was achieved by immersing the fibre in water and deswelling occurred when the wet fibre was removed from the water and exposed to ethanol vapour. The actuation of chitosan is governed significantly by the diffusion of the surrounding fluid into the hydrogel network. The swelling of hydrogels is known to be relatively faster process than the deswelling.[38] Therefore, the coiled fibre was kept in each solution long enough to establish volumetric equilibrium and more time was given for the dehydration stage (5 minutes immersed in water and 10 minutes in ethanol vapour).

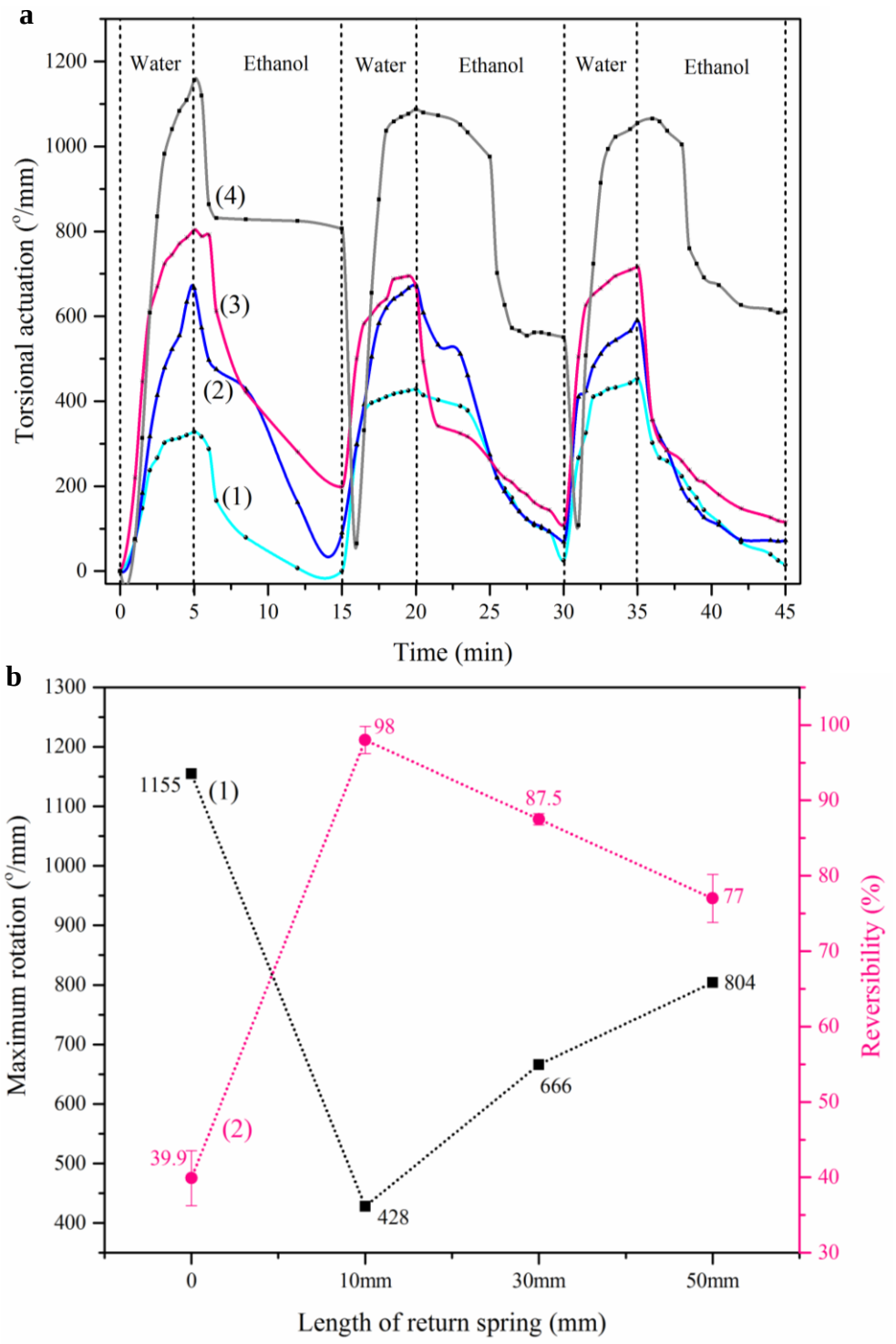

Figure 4 (a) Torsional actuation properties of coiled fibres vs. time using different length of return spring; i.e. (1) 10mm, (2) 30mm, (3) 50mm of return spring used and (4) free torsional actuation (b) comparison of (1) maximum torsional actuation along and (2) reversibility of coiled chitosan fibres using different lengths of return spring (measured values: circles and squares; calculated values: diamonds).

Three different lengths of return spring 10, 30, and 50 mm were used to study their effect on the coiled chitosan torsional rotation. The maximum reversibility shown by a free rotating

coiled fibre was about 45% whilst almost full reversibility was achieved using a 10mm long return spring against the rotating fibre. Longer return spring fibres achieved less reversibility of the water-induced uncoiling (Figure 4 (b)). All return springs decreased the torsional actuation magnitude, as noted previously [41,42] with greater reduction occurring for shorter, torsionally stiffer return spring fibres. Increasing stiffness of shortened return spring provides higher opposing torque to the actuating fibre and a reduced torsional stroke. Here, rotation of the actuating fibre twists the return spring fibre, thereby generating an increasing opposing torque as the sample rotation proceeds. This opposing torque further helps the fibre to be retwisted during the deswelling process.

The effect of the return spring on the torsional actuation can be evaluated in terms of return spring stiffness which proportionally increases as the spring length shortens. Equation ***1*** shows the general expression of fibre torsional stroke when used against a return spring[42] without subjected by other external torque.

$$\phi(\mathrm{L_A})_{\text{return spring}} = \phi(\mathrm{L_A})_{\text{free}} \cdot \left(\frac{S'_A}{S'_A + S_N}\right) \qquad \textit{Equation 1}$$

Here, $\phi(L_A)_{free}$ is torsional stroke at the free end of a one-end-tethered fibre of length L_A, S'_A and S_N are the torsional stiffness of the wet chitosan fibre and the nylon return spring, respectively. Calculated torsional strokes for each return spring length were determined from Equation ***1*** using a linear regression fit and the calculated results were found to compare well with measured values (Figure 5).

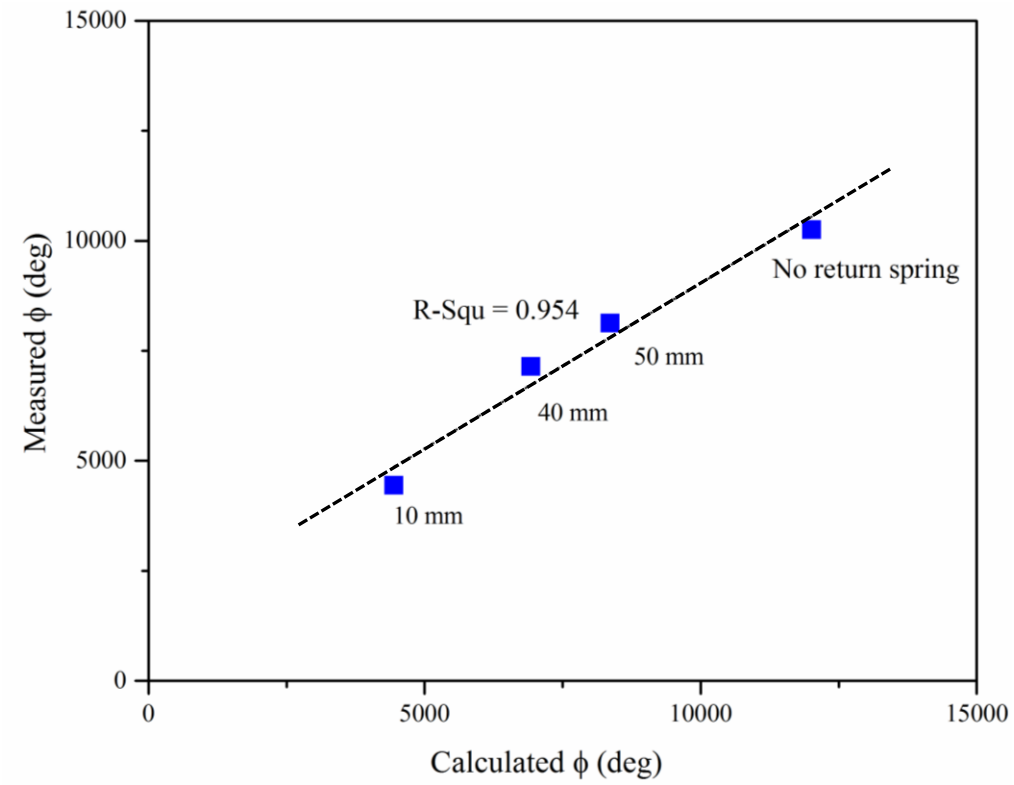

Figure 5 Measured and calculated torsional rotations on hydration of coiled chitosan fibre attached to return springs of the indicated length

High reversibility is desirable in actuator applications, and the two-end-tethered coiled chitosan fibre operated with a 10 mm long return spring generated almost fully reversible torsional actuation of 428º/mm. This amount is close to the highest values among all previous torsional actuators to date. This value is nearly double that of carbon nanotube torsional actuator (250º/mm) [41] and significantly higher than values reported for other torsional actuators based on shape-memory alloys and conducting polymers with produced torsional rotations of 0.15º/mm,[43] and 0.01º/mm,[44] respectively. Figure 6 summarizes and compares previous high stroke torsional actuators. A high torsional rotation of 588º/mm was previously obtained from moisture-activated and coiled graphene fibres,[28] however, these were obtained in the free rotation state so direct comparisons with the chitosan fibre operated against a return spring is difficult.

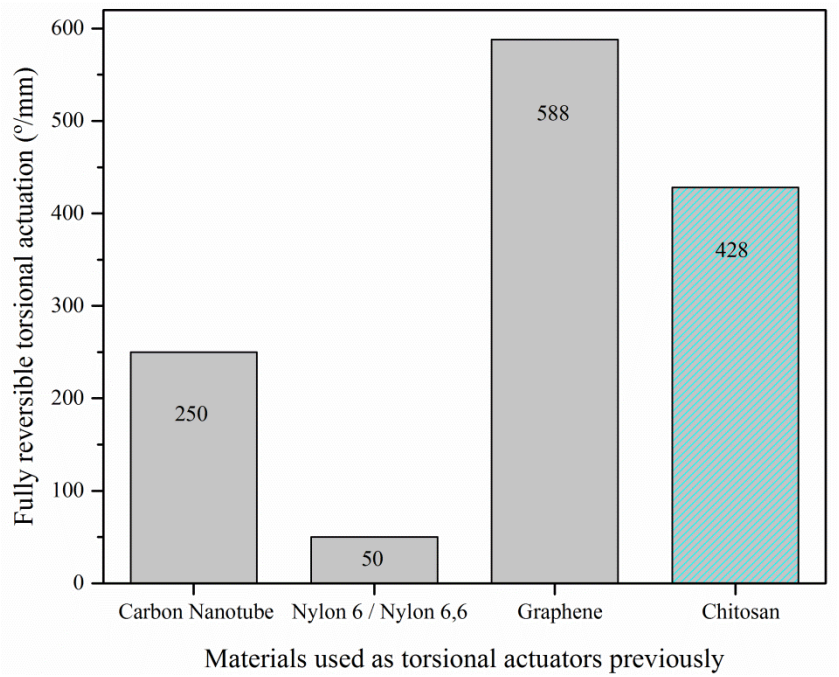

Figure 6 Comparison of performance of previous reversible torsional actuators

3.3.3. Investigation of the mechanism of torsional actuation

Theoretical study of torsional actuation predicts that a given stimulus induces a free rotation that increases in magnitude linearly with fibre length. Equation 4 shows that the actuation stroke also depends on whether the actuation is 'free' or constrained by a return spring. When a return spring is used, the torsional stiffnesses of both the actuating fibre and the return spring become important. When a hydrogel fibre is swollen from it's dry to wet condition, the modulus decreases significantly[45] which also denotes the decrease of torsional stiffness.

Torsional actuation of coiled chitosan fibre can also be analysed based on the helix nature of its coiled structure. Significant changes of fibre volume occur between the wet and dry condition which also drives changes of coil bias angle (defined here in respect to the fibre axis direction). A quantitative theoretical explanation of free torsional stroke can be given from these parameters by the aid of the helix geometry, as illustrated in Figure 7.[46]

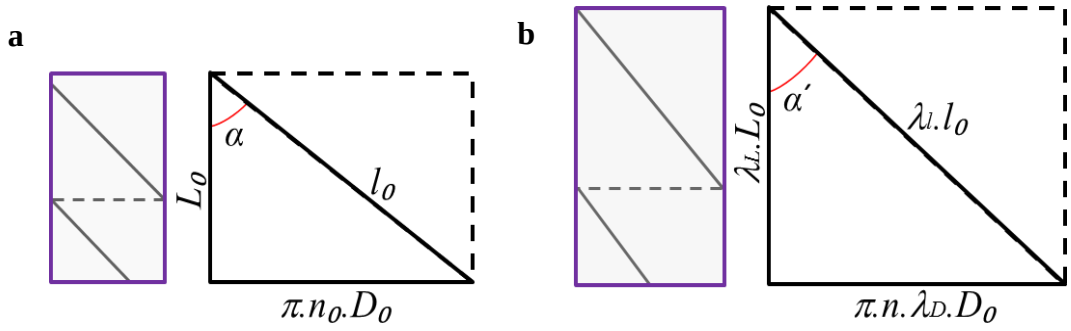

Figure 7 Dimension changes in a coiled chitosan fibre: (a) dry condition; (b) wet condition. L_0 denotes initial coiled fibre length, l_0 is coil helical length, D_0 is initial fibre outer diameter, n_0 and n are the initial and final number of turns in the coil, α and α' denotes the initial and final helix bias angles, and all factors of λ denotes the ratio of the parameter in the wet-state compared to when dry.

The following expressions are obtained from Figure 7 (a) and (b):

$$L_0^2 + \pi^2 . n_0^2 . D_0^2 = l_0^2$$ ***Equation***

$$2\lambda_L^2 . \mathbf{L_0^2} + \boldsymbol{\pi^2 . n^2} . \lambda_D^2 . \mathbf{D_0^2} = \lambda_l^2 . \mathbf{l_0^2}$$

Equation 3

These two equations can be generalized as:

$$\mathbf{n^2} . \lambda_D^2 = \frac{\mathbf{L_0^2}(\lambda_l^2 - \lambda_L^2)}{\boldsymbol{\pi^2 . D_0^2}} + \lambda_l^2 . \mathbf{n_0^2}$$ ***Equation 4***

Stereomicroscopic imaging was conducted to changes in geometry of the coiled chitosan fibre in the dry and wet-states, as shown in Figure 8 and summarized in Table 3. Here, λ_L was calculated considering the length change of a hanging sample attached with a paddle at the free rotating end when subjected to water swelling. The length ratio during hydration of the twisted fibre, λ_l was noted from a separate experiment where the length of a twisted fibre was determined in the dry and wet states. The swelling ratio of the coil diameter from dry to wet (λ_D) was calculated based on the mid-point of the fibre with the procedure illustrated in Figure 8 (c). These swelling ratios were used to estimate the degree of untwist expected in the coiled fibre using Equation 4. For the sample made by overtwisting, the calculation torsional rotation of 868°/mm in the uncoiling direction is in good agreement with the experimental results (675°/mm) in the free rotation condition. Similarly, the mandrel wrapped coil was predicted to have a free uncoiling rotation of 118°/mm, whereas 90°/mm rotation was found experimentally.

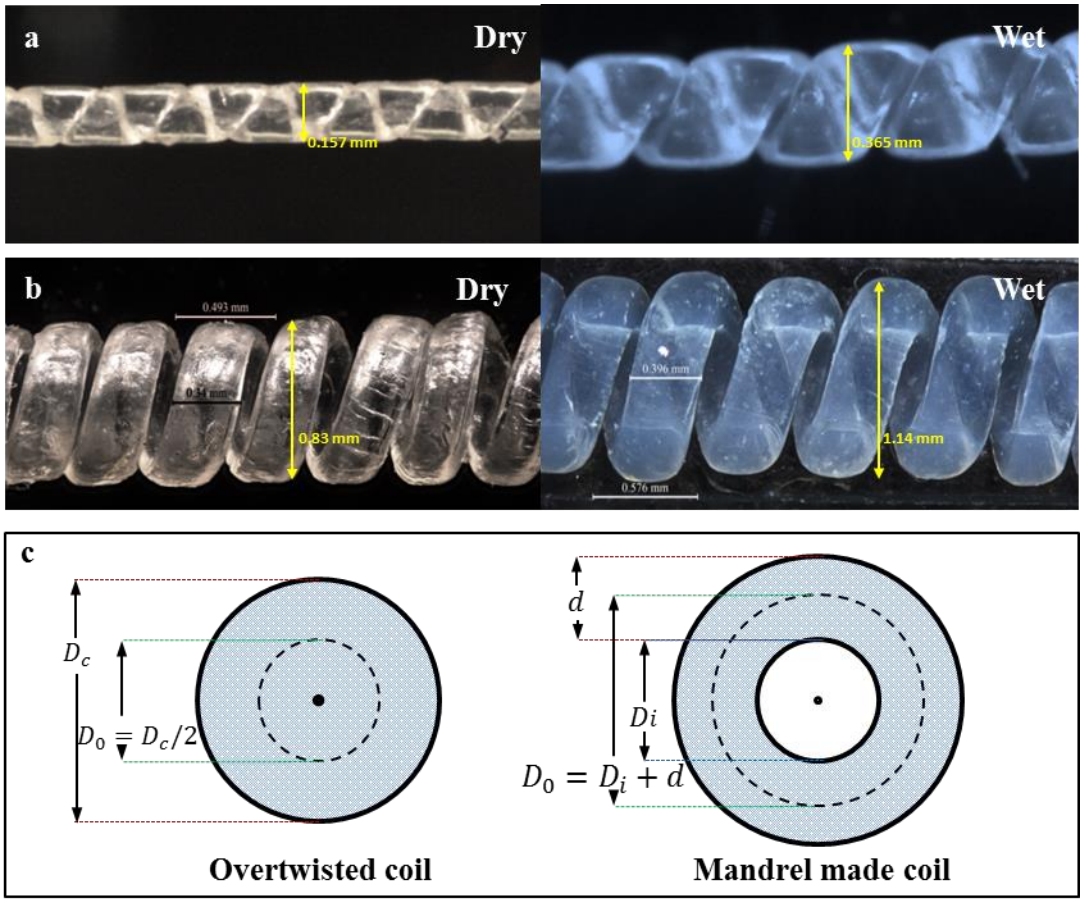

Figure 8 Representative optical microscope images of (a) overtwisted coiled fibre, (b) a mandrel-coiled fibre, in dry and wet-state, respectively; and (c) top view of coiled fibre (D_0=actual coil diameter, D_c=outer diameter of coil, d=fibre diameter incorporated in coil and D_i=internal hollow section of coil).

Table 3 Geometry of coiled chitosan fibre in dry and wet state

	D_0 (mm)	λ_D	L_0 (mm)	λ_L	λ_l
Overtwisted coil	0.0785	0.1825	4	1.097	1.034
Mandrel made coil	0.68	0.89	6	1.16	1.034

3.3.4. In-vitro Bioactivity Experiments

It is well known that the quality of the cell attachment to the materials will determine the capacity of cells to proliferate and differentiate onto the biomaterials.[47,48] To this end, we tested cell attachment and proliferation of our untwisted and coiled fibres using myoblast cells without the need of extra cellular matrices such as laminin and collagen to assess the true affinity of cells to our materials. The test revealed that on both untwisted and coiled chitosan fibres the myoblast cells attached, differentiated and proliferated with in the 5 days tested as observed in Figure 9.

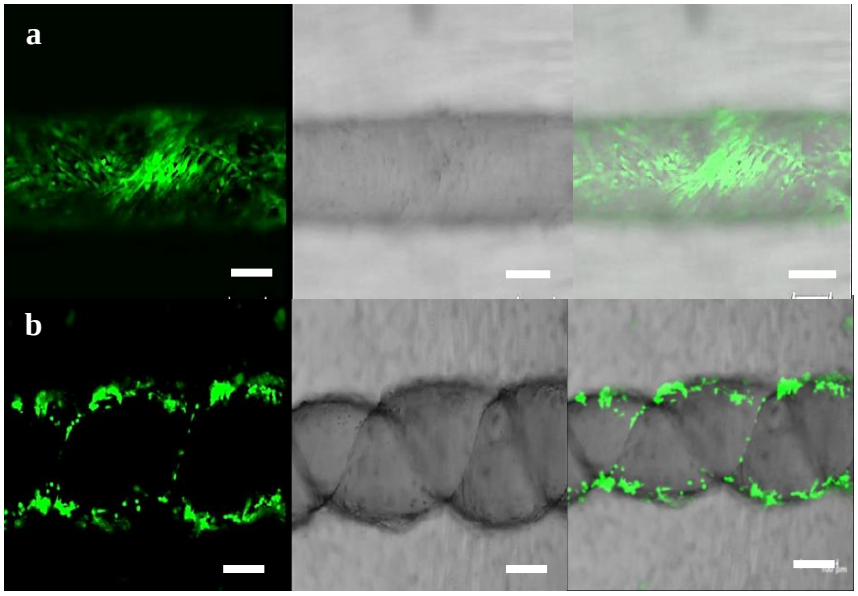

Figure 9 Skeletal muscle cell attachment and proliferation on fibres after 4 days of differentiation. (a) chitosan and (b) Twisted chitosan fibres. Scale bars represent 100 µm

The cell morphology after 5 days on the fibres it appears to be typical of myoblast cells. It was observed that cells attached slightly better on the untwisted fibres than on the coiled ones as showed in Figure 9, perhaps due to the fibre's shape. Overall, the myoblast cells were observed to adhere, and the density of cells on the fibres increased over the 5 days tested, indicating that the fibres were capable of supporting myoblast cell adhesion and proliferation. These results indicated that the fibres did not release any chemical used during fabrication (no toxic) suggesting that our fibres are biocompatible.

Mechanical stimulation especially stretching has demonstrated to have a vital control over cell morphology and proliferation and differentiation enhancement has demonstrated to improve tissue-engineered human skeletal muscle at the cellular levels, as previously discussed.[22,23] Considering cells' tendency toward adhering and growing on the fibres and the fact that torsional actuation would act as a mechanical action (both tension *via* swelling and torsion *via* rotation), a schematic cell culture model could be proposed to study and predict the changes in cell responses upon receiving mechanical signals (torsional actuation) as demonstrated in Figure 10.

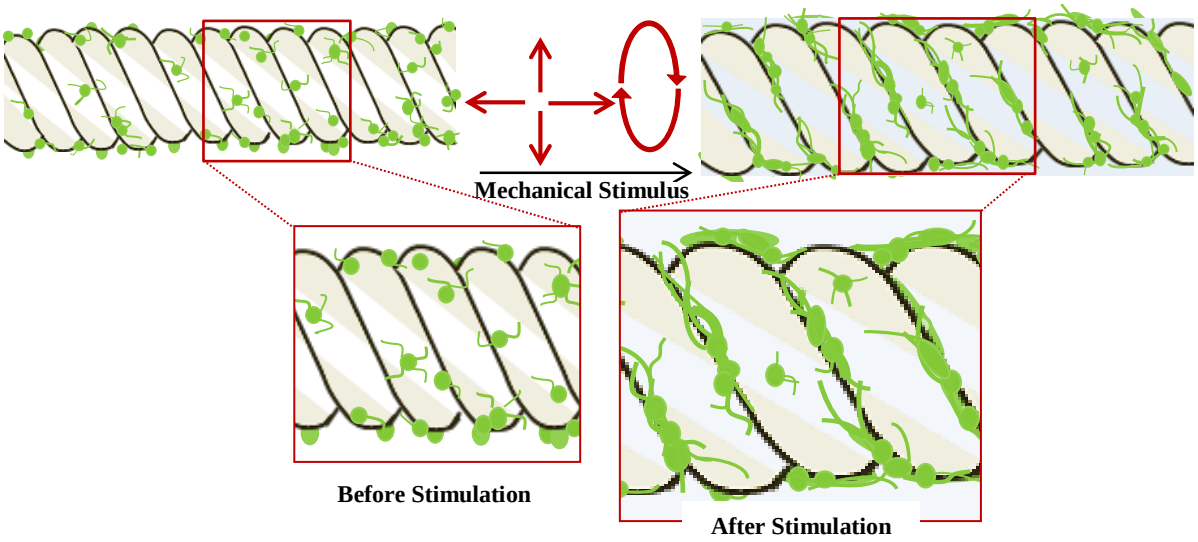

Figure 10 A schematic cell culture model suggest attachment and growth of cell upon mechanical stimulation

As could be seen in Figure 10, it is suggested that cell growth and differentiation can be guided by mechanical stimuli through a so-called mechanotransduction mechanism. Therefore, it could be imagined that after applying different mechanical stimuli, cells differentiation will be improved especially on sites more exposed by mechanical signals such as coil junctions.

Conclusions

High performance biofibres as artificial muscles have been demonstrated for the first time using wet-spinning processes. Highly coiled wet-spun chitosan fibres could provide partially reversible and large torsional actuation behaviour when hydrated. Adding a return spring fibre decreased the amount of torsional actuation while increase the percentage of reversibility depending upon the return spring length. SEM images of the cross-section of coiled chitosan fibres showed permanent helical structure of those after drying with diameters of ~190±10 µm. Investigation of mechanical properties showed a significant decrease in robustness of the coiled fibres compared to twisted and neat fibres. The moisture-activated torsional behaviour of twist-spun chitosan structures has shown to give significant values up to 1155˚/mm. The single helix model was used to evaluate the mechanism of torsional actuation of coiled chitosan fibres. The cytocompatiblity of as-prepared fibres muscles was evaluated by using skeletal muscle cell line. These properties are essential for studies involving the use of mechanical stimulation to promote nerve regrowth and/or muscle regeneration. Unique combination of partially reversible torsional actuation and acceptable

mechanical properties of these fibres make them potentially applicable as self-powered biofibres actuators for developing artificial muscles.

Acknowledgements

This work was supported by funding from the University of Wollongong, Australian Research Council Centre of Excellence and Laureate Fellowships (G. G. Wallace) and the Australian Research Council under Discovery Early Career Researcher award (Javad Foroughi DE12010517). The authors would also like to thank Saber Mostafavian for the 3D set-up design. Mr. Rodrigo Lozano also would like to acknowledge the support of the Consejo Nacional de Ciencia y Tecnologia (CONACYT, Mexico).

References

1 Z. Suo, *Acta Mech. Solida Sin.*, 2010, **23**, 549–578.

2 T. Mirfakhrai, J. D. W. Madden and R. H. Baughman, *Mater. Today*, 2007, **10**, 30–38.

3 B. T. F. Otero and J. M. Sansin, *Adv. Mater.*, 2015, **4095**, 491–494.

4 L. B. A. Č. Áková, E. Filová, F. R. Č. Ek, V. Š. Č. Ík and V. Starý, *Physiol. Res.*, 2004, **53**, S35–S45.

5 M. F. Maitz, U. Freudenberg, M. V Tsurkan, M. Fischer, T. Beyrich and C. Werner, *Nat Commun*, 2013, **3168**, 1–8.

6 H. Geckil, F. Xu, X. Zhang, S. Moon and U. Demirci, *Nanomedicine*, 2011, **5**, 469–484.

7 F. Carpi, R. Kornbluh, P. Sommer-larsen and G. Alici, *Bioinsp. Biomim.*, 2011, **6**, 045006.

8 J. M. G. Swann and A. J. Ryan, *Polym Int*, 2009, **58**, 285–289.

9 B. Y. Osada and J. Gong, *Adv. Mater*, 1998, **10**, 827–837.

10 A. S. Chen, Guohua;Hoffman, *Nat.*, 1995, **373**, 49–52.

11 S. Kaewpirom and S. Boonsang, *Eur. Polym. J.*, 2006, **42**, 1609–1616.

12 L. Ionov, *Biochem. Pharmacol.*, 2014, **17**, 494–503.

13 D. Trivedi, C. D. Rahn, M. Kier and I. D. Walker, *Appl. Bionic. Biomech.*, 2008, **5**, 99–117.

14 E. W. H. Jager, in *Proc. of SPIE Vol.*, 2012, vol. 8340, pp. 1–10.

15 S. K. De, N. R. Aluru, B. Johnson, W. C. Crone, D. J. Beebe and J. Moore, *J. Microelectromech. Syst.*, 2002, **11**, 544–555.

16 Y. Forterre, *J. Exp. Bot.*, 2013, 6pp.

17 P. Chen, Y. Xu, S. He, X. Sun, S. Pan, J. Deng, D. Chen and H. Peng, *Nat. Nanotechnol.*, 2015, 1–8.

18 J. Wang, G. Wang, X. Feng, T. Kitamura, Y. Kang, S. Yu and Q. Qin, *Sci. Rep.*, 2013, **3**, 1–7.

19 N. Plaza, S. L. Zelinka and D. S. Stone, *Smart Mater. Struct. 22*, 2013, **22**.

20 Q. Guo, E. Dai, X. Han, S. Xie, E. Chao and Z. Chen, *Interface*, 2015, **12**.

21 M. J. Berridge, *J Physiol*, 2008, **21**, 5047–5061.

22 T. Constructs, 2012, **18**, 288–300.

23 C. A. Powell, B. L. Smiley, J. Mills, H. H. Vandenburgh, A. Courtney, B. L. Smiley, J. Mills and H. H. Vandenburgh, *Am J Physiol Cell Physiol*, 2002, **283**, 1557–1565.

24 K. S. Kang, S. Lee and H. Lee, *Exp. Mol. Med.*, 2011, **43**, 367–373.

25 T. M. Maul and D. W. Chew, *Biomech Model Mechanobiol. Author*, 2012, **10**, 939–953.

26 T. P. Lele, J. E. Sero, B. D. Matthews, S. Kumar, S. Xia, M. Montoya-zavala, T. Polte, D. Overby, N. Wang and D. E. Ingber, in *METHODS IN CELL BIOLOGY*, 2007, pp. 443–472.

27 M. D. Lima, G. M. Spinks, M. E. Kozlov, C. S. Haines, D. Suh, J. Foroughi, S. J. Kim, Y. Chen, T. Ware, M. K. Shin, L. D. Machado, A. F. Fonseca, J. D. W. Madden, W. E. Voit, D. S. Galvão and R. H. Baughman, *Science (80-.).*, 2012, **928**, 928–932.

28 H. Cheng, Y. Hu, F. Zhao, Z. Dong, Y. Wang and N. Chen, *Adv. Mater. 2014*, 2014, **26**, 2909–2913.

29 J. S. Moore, J. M. Bauer, Q. Yu, R. H. Liu, C. Devadoss and B. Jo, *Nat.*, 2000, **404**, 588–590.

30 J. M. Karp, Y. Yeo, W. Geng, C. Cannizarro, K. Yan, D. S. Kohane, G. Vunjak-novakovic, R. S. Langer and M. Radisic, *Biomater.*, 2006, **27**, 4755–4764.

31 J. C. Cheng, S. Member and A. P. Pisano, *J. Microelectromech. Syst.*, 2008, **17**, 402–409.

32 A. Agrawal, N. Wanasekara, V. Chalivendra, N. Rahbar and P. Calvert, in *Bioengineering Conference (NEBEC)*, 2011, pp. 6–7.

33 M. Hu, R. Deng, K. M. Schumacher, M. Kurisawa, H. Ye, K. Purnamawati and J. Y. Ying, *Biomater.*, 2010, **31**, 863–869.

34 R. M. Quigley, A. F., Kita, M., Cornock, R., Mysore, T., Foroughi, J., Wallace, G. G. & Kapsa, in *Fiber Society Spring Technical Conference*, 2013, pp. 252–253.

35 M. Dash, F. Chiellini, R. M. Ottenbrite and E. Chiellini, *Prog. Polym. Sci.*, 2011, **36**,

981–1014.

36 A. Mirabedini, J. Foroughi, T. Romeo and G. G. Wallace, *Macromol. Mater. Eng.*, 2015, **300**, 1217–1225.

37 Y. A. Ismail, S. R. Shin, K. M. Shin, S. G. Yoon, K. Shon, S. I. Kim and S. J. Kim, *Sens. Actuators, B*, 2008, **129**, 834–840.

38 S. Enrique and L. Larios, University of Wollongong, 2009.

39 C. S. Haines, M. D. Lima, N. Li, G. M. Spinks, J. Foroughi, J. D. W. Madden, S. H. Kim, S. Fang, M. J. D. Andrade, F. Göktepe, Ö. Göktepe, S. M. Mirvakili, S. Naficy, X. Lepró, J. Oh, M. E. Kozlov, S. J. Kim, X. Xu, B. J. Swedlove, G. G. Wallace and R. H. Baughman, *Science (80-.).*, 2014, **343**, 868–872.

40 K. J. Gilmore, M. Kita, Y. Han, A. Gelmi, M. J. Higgins, S. E. Moulton, G. M. Clark, R. Kapsa and G. G. Wallace, *Biomaterials*, 2009, **30**, 5292–5304.

41 J. Foroughi, G. M. Spinks, G. G. Wallace, J. Oh, M. E. Kozlov, S. Fang, T. Mirfakhrai, J. D. W. Madden, M. K. Shin, S. J. Kim and R. H. Baughman, *Science (80-.).*, 2011, **334**, 494–498.

42 S. Aziz, S. Na, J. Foroughi, H. R. Brown and G. M. Spinks, *Polym. Test.*, 2015, **46**, 88–97.

43 A. C. Keefe and G. P. Carman, *Smart Mater. Struct.*, 2000, **9**, 665–672.

44 Y. Fang, T. J. Pence and X. Tan, *IEEE/ASME Trans. Mechatron.*, 2011, **16**, 656–664.

45 R. Wu, R. A. Niamat, B. Sansbury and M. Borjigin, *Fibers*, 2015, **3**, 296–308.

46 S. Aziz, S. Naficy, J. Foroughi, H. R. Brown and G. M. Spinks, *J. Polym. Phys. B*, 2016, **54**, 1278–1286.

47 K. Anselme, *Biomaterials*, 2000, **21**, 667–681.

48 A. Mirabedini, J. Foroughi, B. Thompson and G. G. Wallace, *Adv. Eng. Mater.*, 2015, **18**, 284–293.